STAR Protocols

CellPress
OPEN ACCESS

Protocol

Protocol for matching protein localization to synapse morphology in primary rat neurons by correlative super-resolution microscopy

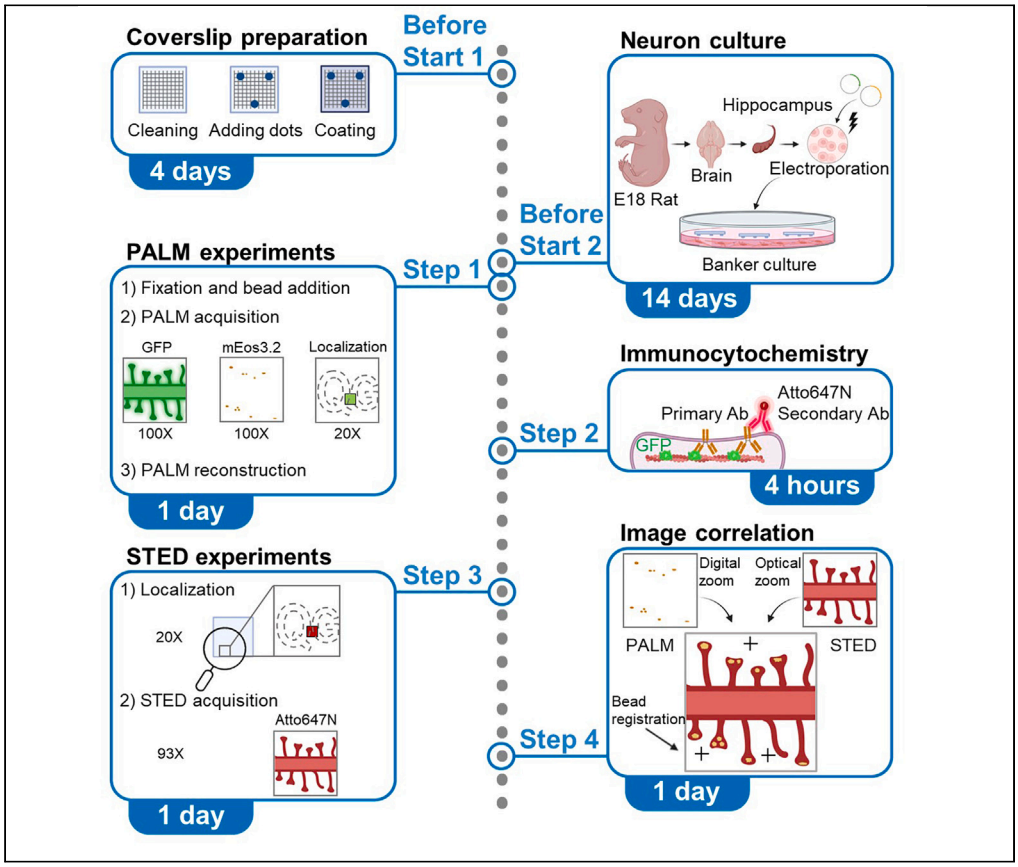

Super-resolution imaging provides unprecedented visualization of sub-cellular structures, but the two main techniques used, single-molecule localization microscopy (SMLM) and stimulated emission depletion (STED), are not easily reconciled. We present a protocol to super-impose nanoscale protein distribution reconstructed with SMLM to sub-cellular morphology obtained in STED. We describe steps for tracking cells on etched coverslips and registering images from two different microscopes with 30-nm accuracy. In this protocol, synaptic proteins are mapped in the dendritic spines of primary neurons.

Publisher's note: Undertaking any experimental protocol requires adherence to local institutional guidelines for laboratory safety and ethics.

Tiffany Cloâtre, Magali Mondin, Jean-Baptiste Sibarita, Florian Levet, Olivier Thoumine

florian.levet@u-bordeaux.fr (F.L.)
olivier.thoumine@u-bordeaux.fr (O.T.)

Highlights

Instructions for imaging specific synaptic proteins with PALM in primary neurons

Guidance on imaging dendritic spines immunostained for actin with STED

Steps for correlating PALM and STED images acquired on two different microscopes

Procedures for mapping synaptic proteins within the volumes of dendritic spines

Cloâtre et al., STAR Protocols 5, 103160
September 20, 2024
https://doi.org/10.1016/j.xpro.2024.103160

STAR Protocols

CellPress
OPEN ACCESS

Protocol

Protocol for matching protein localization to synapse morphology in primary rat neurons by correlative super-resolution microscopy

Tiffany Cloâtre,[1,3] Magali Mondin,[2] Jean-Baptiste Sibarita,[1] Florian Levet,[1,2,*] and Olivier Thoumine[1,4,*]

[1]University Bordeaux, CNRS, Interdisciplinary Institute for Neuroscience, IINS, UMR 5297, 33000 Bordeaux, France

[2]University Bordeaux, CNRS, INSERM, Bordeaux Imaging Center, BIC, UAR 3420, US 4, 33000 Bordeaux, France

[3]Technical contact

[4]Lead contact

*Correspondence: florian.levet@u-bordeaux.fr (F.L.), olivier.thoumine@u-bordeaux.fr (O.T.)
https://doi.org/10.1016/j.xpro.2024.103160

SUMMARY

Super-resolution imaging provides unprecedented visualization of sub-cellular structures, but the two main techniques used, single-molecule localization microscopy (SMLM) and stimulated emission depletion (STED), are not easily reconciled. We present a protocol to super-impose nanoscale protein distribution reconstructed with SMLM to sub-cellular morphology obtained in STED. We describe steps for tracking cells on etched coverslips and registering images from two different microscopes with 30-nm accuracy. In this protocol, synaptic proteins are mapped in the dendritic spines of primary neurons.

For complete details on the use and execution of this protocol, please refer to Inavalli et al.[1]

BEFORE YOU BEGIN

This protocol describes how to acquire images of the same cell sample in two different super-resolution microscopy modes, specifically SMLM and STED, and correlate them at a 30-nm precision. This strategy allows one to super-impose the localizations of specific molecular components onto images of cellular structures, in our case the distribution of the post-synaptic density protein PSD-95 within the shape of dendritic protrusions delineated by the actin cytoskeleton, in primary cultures of rat hippocampal neurons. We have also used this protocol to correlate dSTORM images with STED images.

Institutional permissions

To prepare dissociated neuronal cultures from E18 rat embryos, gestant Sprague-Dawley rat females were handled and sacrificed according to European ethical rules and recommendations from the local ethics committee from the University of Bordeaux (EC50).

Preparation of etched coverslips

Timing: 3 h over a 4 days period

This section describes how to clean and coat coverslips prior to neuron plating.

1. Coverslip cleaning.

a. Using tweezers, place the 18 mm square coverslips one by one in appropriate ceramic racks (Figure 1A). Set the racks in rectangular staining tanks or jars containing nitric acid for 16 h to wash the coverslips (Figure 1B).

⚠ CRITICAL: Perform this step in a chemical fume hood with lab coat and nitrile gloves, and dispose of acid in appropriate waste containers.

Note: Alternatives to nitric acid can be used to clean the coverslips, including solvents such as acetone or methanol, and concentrated bases such as potassium hydroxide.

b. Remove racks with coverslips from nitric acid. Set the racks in other staining tanks dedicated to water rinses, and rinse 6 times for at least 30 min each with milliQ water.
c. Use absolute ethanol for one final rinse of 30 s before sterilization.
d. Remove and discard the ethanol.
e. Put racks with coverslips in an empty crystallizer dish covered with an aluminum foil for sterilization in a dry oven, at 240°C for 8 h (Figure 1C).

⚠ CRITICAL: Perform this step just after the ethanol wash.

f. Under a laminar flow hood and using sterile forceps, place 2 etched coverslips onto the bottom of one 60-mm tissue culture plastic dish (neuron dishes).

⚠ CRITICAL: Coverslips must not overlap each other.

g. Using a shelf microscope, check that the numbers and letters on the etched coverslips are correctly oriented. Otherwise, turn the coverslips upside down under the hood.

2. Deposition of paraffin dots on the coverslips.
   a. Put the paraffin in a 100-mL bottle, and place it in a 250-mL beaker containing water (waterbath).
   b. Place the beaker containing the paraffin bottle in an oven at 150°C for at least 1 h before use.
   c. Under a sterile hood, plunge a sterile plugged 230-mm Pasteur pipette in the paraffin and place three paraffin dots per coverslip previously prepared in 60-mm dishes (Step 1f).

⚠ CRITICAL: Place the dots not too close to the edges of the coverslips.

⚠ CRITICAL: Put back the paraffin in the oven when it starts to solidify.

Pause point: Coverslips can be kept for a few weeks in a clean environment before coating.

3. Coverslips coating with Poly-L-Lysine (PLL).
   a. Dilute PLL at 1 mg/mL in borate buffer.
   b. Sterilize with a 0.22-µm filtration unit.
   c. Put 300 µL of PLL solution on each coverslip.
   d. Incubate for 16 h at 37°C.
   e. Rinse coverslips twice with 5-mL sterile milliQ water.
   f. Add 5 mL of plating medium per dish.
   g. Set in the 37°C - 5% CO2 incubator at least 24 h before seeding neurons, to allow for pH equilibration.

Preparation of glial cell dishes

Timing: 3 × 15 min, 2 weeks and 24 h before seeding neurons

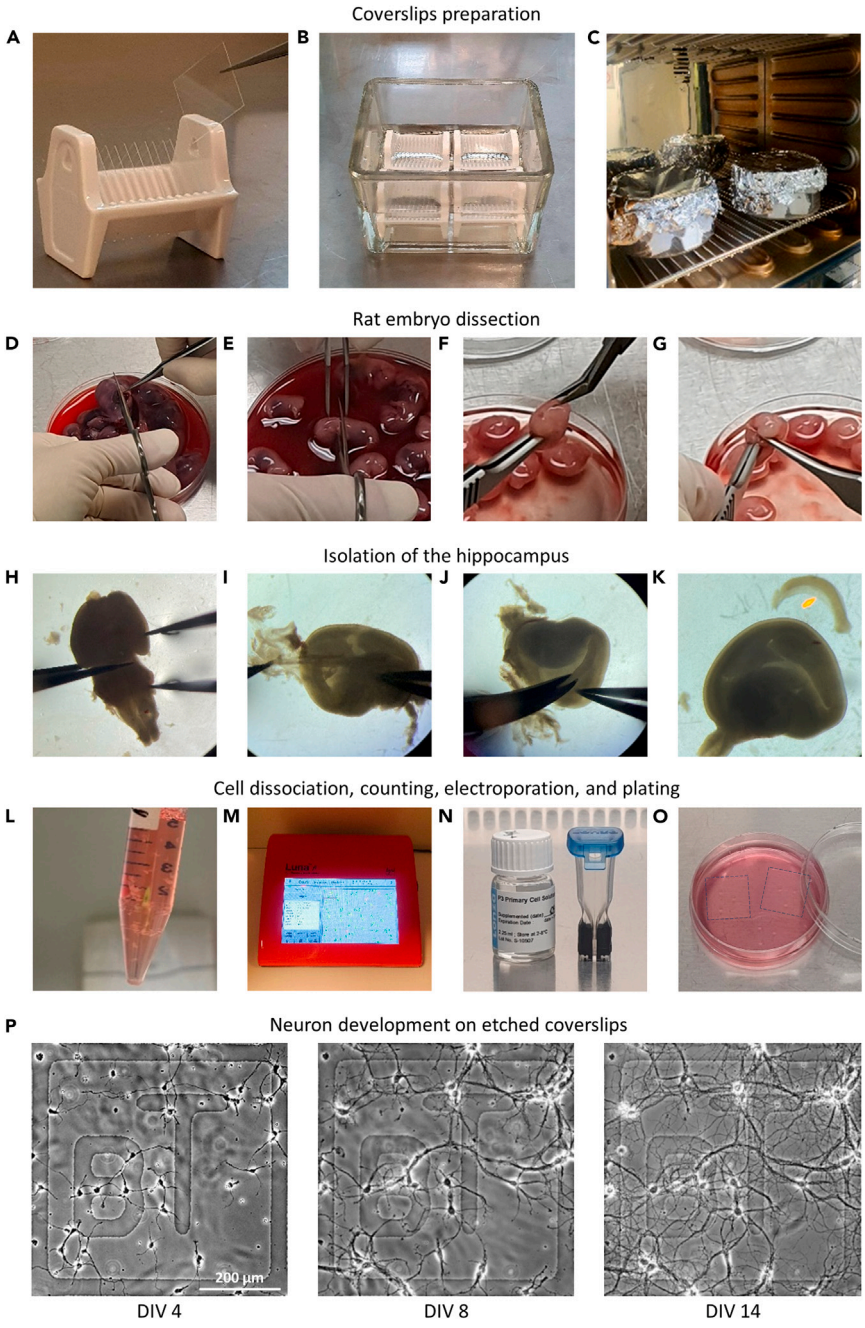

Figure 1. Banker culture of primary rat hippocampal neurons on etched coverslips

(A–C) Photographs showing respectively an individual ceramic rack containing etched coverslips, a staining tank containing 4 ceramic racks and filled with cleaning or rinsing solution, and the sterilization process in an oven at 240°C.

(D–G) Photographs of the different steps of the dissection of rat embryos, leading to brain extraction.

(H–K) Successive steps of hippocampus isolation.

(L–O) Photographs showing respectively a 15 mL tube containing the hippocampi being digested in trypsin solution, the cell counting device, the electroporation solution and cuvette, and 2 PLL-coated etched coverslips seeded with neurons and placed in a 60 mm culture dish previously covered with a glial cell monolayer.

(P) Bright field images of hippocampal neurons growing on etched coverslips, taken at different developmental times (DIV 4, 8, and 14). Note the etched pattern BT within the 500 µm square in the same field of view. After 14 days *in vitro* (DIV), neurons are fixed, labeled, and processed for correlative super-resolution microscopy.

This section describes how to culture glial cells on plastic dishes that serve as a feeder layer to neurons plated on glass coverslips. Glial cells and neurons are actually prepared from the same dissection of embryonic rat hippocampi described in detail in steps 7–9 below, but neurons are placed in contact with glial cell layers that were made two weeks earlier.

4. Coating of glial cells dishes.
   a. Dilute PLL at 0.1 mg/mL in borate buffer.
   b. Sterilize with a 0.22-μm filtration unit.
   c. Put 1 mL of PLL solution in each individual 60-mm dish.
   d. Incubate for 2 h at 37°C.
   e. Rinse dishes twice with 5-mL sterile milliQ water.
   f. Add 5 mL of plating medium per dish.
   g. Set in the 37°C - 5% CO2 incubator at least 24 h before seeding cells, to allow for pH equilibration.

   Note: The coating of glass coverslips for neurons and glial cell dishes can be made in parallel using the same PLL stock solution.

5. At the end of the dissection (see Step 9i).
   a. Plate glial cells on PLL-coated 60 mm plastic dishes at a density of 20,000 cells per dish in 5 mL plating medium.
   b. Leave them in the 37°C - 5% CO_2 incubator for 2 weeks.

   Note: Under these culture conditions, glial cells proliferate while neurons do not survive, such that glial cells finally form a 80-90% confluent monolayer on the plastic surface. Glial cells are then ready to serve as a feeder layer to neurons prepared 2 weeks later. Glial cells can be used fresh, or frozen in DMEM + 10% DMSO, stored in liquid nitrogen, and thawed for later use for example when a dissection is not optimal or after interruptions in the culture pipeline.

6. Medium change of the 14 days old glia dishes, to be performed at least 24 h before the dissection.
   a. Remove the plating medium from the 2-week old glial cell dishes.
   b. Rinse cells with 2 mL of warm feeding medium and add 5 mL of the same medium.
   c. Put the dishes back in the 37°C-5% CO_2 incubator.

Dissection, electroporation and culture of primary neurons

Timing: 3 h, 2 weeks before imaging experiments

This section describes the different steps to dissociate individual cells from embryonic rat hippocampi, to electroporate them, and to culture neurons and glial cells on their respective substrates. The whole procedure is based on an established protocol.[2]

7. Rat embryo dissection and brain extraction (Figures 1D–1G).
   a. Thaw at 22°C one aliquot of trypsin solution (5 mL) and one aliquot of horse serum (3 mL).
   b. Anesthetize a pregnant rat female with CO_2, complying to national ethical regulations for the handling of animals.
   c. Sterilize abdomen with 70% ethanol.
   d. Grip the skin with wide-tipped forceps, cut the skin and the muscles along the midline with surgical scissors.
   e. Make two cuts to the sides and pull out both horns of the uterus. Detach the uterus and transfer it to a 100-mm tissue culture dish.

⚠ CRITICAL: From this step on, proceed sterilely under a dissection hood.

f. Cover the uterus with 15 mL of cold dissection buffer previously kept on ice.
g. Open the uterus with fine scissors (Figure 1D). Remove the embryos and decapitate them immediately with sharp scissors (Figure 1E). Place heads in a 60-mm dish containing 5 mL of cold dissection buffer.
h. Using curved forceps, hold one head firmly by inserting the tips of the forceps into the orbits. Using spring angled scissors, carefully cut through the skin and skull from the point of decapitation towards the orbits (Figure 1F).
i. Using straight and fine forceps, remove the intact brain and place it in a 35-mm dish containing 3 mL of cold dissection buffer (Figure 1G).

8. Hippocampi isolation.
   a. Under a binocular microscope, separate the hemispheres of the brain by moving Dumont forceps through the midline (Figure 1H).
   b. Carefully remove the meninges and choroid plexus (Figure 1I).

Note: The meninges form a thin layer covering the surface of the brain. The choroid plexus attaches to the meninges at the edge of the hippocampus. Both of these layers are highly vascularized, which facilitates locating and removing them.

⚠ CRITICAL: Efficient removal of the meninges and choroid plexus prevents the growth of fibroblasts and other unwanted cell types, ensuring a more homogenous population of neurons.

   c. One hemisphere at a time, remove the septum, thalamus, and hypothalamus from the cortex to expose the hippocampus, which will appear curved along the medial edge of the cortex.
   d. Remove the olfactory bulb and striatum to further expose the hippocampus for easy removal.
   e. Using spring curved scissors, separate the hippocampus from the rest of the brain (Figure 1J), and place it in a 35-mm dish containing 3 mL of cold dissection buffer (Figure 1K).

⚠ CRITICAL: There are also meninges specifically associated with the hippocampus, whose removal is highly recommended as well.

   f. Repeat steps 8c-e with the other hemisphere, then repeat the entire procedure with the remaining brains. Place all isolated hippocampi in the same 35-mm dish.

9. Cell dissociation and pre-plating.
   a. Transfer all hippocampi and dissection medium with a 150-mm Pasteur pipette of 1.3-mm bore size or with the forceps in a 15-mL conical tube (Figure 1L). After sedimentation, remove the supernatant.
   b. Add 5 mL of the previously thawed trypsin solution. Incubate for 15 min at 37°C in a water-bath.
   c. Remove the trypsin solution.
   d. Rinse hippocampi twice for 5 min by adding 5 mL of dissection buffer, and leave 2 mL.
   e. Triturate tissue gently with a fire-polished 150-mm Pasteur pipette of 0.75-mm bore size or with a 200 µL tip coated with the previously thawed horse serum (HS) until hippocampi appear entirely dissolved (count around 20 strokes).

Note: Pipette coating consists in 2–3 back and forth aspirations of the HS, and is necessary for the cells not to adhere to inside walls of the pipette.

   f. Triturate the suspension with a pipette of 0.5-mm bore size coated with HS until remaining pieces of tissue are broken up and the solution appears cloudy.
   g. Transfer the cells in a 2-mL microtube. Mix 18 µL of the cell suspension with 2 µL of acridine orange/propidium iodide stain solution and count the cells with an automated fluorescence cell counter LUNA-FL (Figure 1M) or any other counting device such as a Malassez hemocytometer.

Note: A single hippocampus contains approximately 500,000 cells.

h. Add 75,000 cells per dish in neuron dishes for pre-plating.
i. Add 20,000 cells per dish in glia dishes previously filled with 5 mL of plating medium (see step 5).

Note: Glia dishes will be used 2-weeks later to receive the glass coverslips freshly plated with neurons (see steps 4–6).

10. Electroporation
    a. For each electroporation, place 300 μL of RPMI medium in a 1.5 mL microtube and 3 mL of DMEM + 10% HS in a 15 mL conical tube, and heat them up to 37°C in a water bath.
    b. Put 300,000 cells from the freshly prepared suspension (Step 9f) in the 15 mL tube containing DMEM-HS and centrifuge this cell suspension for 5 min at 194 × *g*.
    c. Prepare a mix of plasmids (5 μg total DNA) in a 1.5 mL microtube (here 2.5 μg GFP-actin[3] and 2.5 μg Xph20-mEos3.2, an intrabody to the post-synaptic protein PSD-95,[4,5] or 2.5 μg of mEos3.2-actin[1,6]).
    d. Remove the supernatant and resuspend the cell pellet with 100 μL of P3 primary cell nucleofector solution (Figure 1N).

    Note: The solution should be brought to 22°C before use.

    e. Mix this neuron suspension with the 5 μg plasmid mix in the 1.5 mL microtube.
    f. Transfer all suspensions in the Nucleocuvette Vessel and proceed for electroporation in the 4D-Nucleofector X Unit.
    g. Add 300 μL of RPMI medium in the Nucleocuvette Vessel (Figure 1N) and transfer the whole suspension into a sterile 1.5 mL microtube using the plastic pipette included in the manufacturer's kit.
    h. Leave the tube for 5 min in the 37°C-5% CO_2 incubator.
11. Neuron seeding and Banker culture.
    a. Pipet the 300,000 electroporated neurons into the neuron dishes containing the etched coverslips and add 75,000 non-electroporated neurons, previously kept in the incubator (Figure 1O).

    Note: The presence of non-electroporated neurons promotes the survival and development of electroporated neurons.

    b. Two hours after plating to allow for the neurons to adhere to the coverslips, flip the coverslips from one neuron dish into one 2-week old glia dish (the paraffin dots serving as spacers are now facing down).
    c. Three days after flipping, add 10 μL of 1 mM Ara-C stock solution per neuron dish (final concentration 2 μM).

    Note: Ara-C is an antimitotic drug that blocks cell division, and is thus used to prevent the proliferation of glial cells on the coverslips, so that there is an almost pure population of neurons to examine.

    d. Once a week, replace 1 mL of the medium with warm pre-equilibrated feeding medium.
    e. Use neurons at DIV 14–15 when synapses are well established and cultures are robust (Figure 1P).

    Note: Cells can be maintained in those cultures for up to 3 weeks. During this time period, neurons gradually extend axons and dendrites and form synapses between them in a critical period around DIV 8–12.

⚠ CRITICAL: Always keep the neurons covered with medium, as they are extremely sensitive to air and will die if they lack humidity, even briefly.

Preparation of buffers

Timing: 1 day

This section describes the recipes for preparing the buffers used in this protocol.

Buffers for neuron culture can be prepared in advance according to the recipes given in[7] and stored at 4°C. Buffers for correlative microscopy should be prepared shortly before the experiments.

⚠ CRITICAL: Work in sterile conditions for cell culture. Solutions for immunostainings should be prepared fresh and cannot be kept thereafter.

KEY RESOURCES TABLE

REAGENT or RESOURCE	SOURCE	IDENTIFIER
Antibodies		
Mouse anti-GFP (1:1000)	Roche	Cat# 11814460001; Clone 7.1 and 13.1 RRID:AB_390913
Goat anti-mouse Atto-647N (1:500)	Sigma-Aldrich	Cat# 50185 RRID:AB_1137661
Chemicals, peptides, and recombinant proteins		
Nitric acid	Sigma-Aldrich	Cat# 7697-37-2
RPMI 1640 medium Gibco	Thermo Fisher Scientific	Cat# 11875101
Neurobasal plus medium	Thermo Fisher Scientific	Cat# A3582901
B27 plus 50×	Thermo Fisher Scientific	Cat# A3582801
Dulbecco's modified Eagle's medium (DMEM)	Eurobio	Cat# L0106-500
Trypsin-EDTA (0.05%), phenol red	Thermo Fisher Scientific	Cat# 25300054
Poly-L-lysine	Sigma-Aldrich	Cat# P2636
Paraformaldehyde, PFA (powder)	Prolabo	Cat# 28794.295
Horse serum	Thermo Fisher Scientific	Cat# 26050088
NaCl	Sigma-Aldrich	Cat# S7653
HEPES powder	Sigma-Aldrich	Cat# H4034
HEPES buffer 1 M	Thermo Fisher Scientific	Cat# 15630056
D-glucose	Euromedex	Cat# UG3050-A
$MgCl_2$ $(H_20)_6$	Sigma-Aldrich	Cat# M9272
KCl	Sigma-Aldrich	Cat# P4504
$CaCl_2$ $(H_20)_2$	Sigma-Aldrich	Cat# C7902
NH_4Cl	Sigma-Aldrich	Cat# A-4514
BSA fraction V biotin free	Carl Roth	Cat# 0163.4
Glycerol	Sigma-Aldrich	Cat# G5516
Phosphate-buffered saline (PBS) 10×	Euromedex	Cat# ET330-A
Sucrose	Sigma-Aldrich	Cat# S9378
Fluorescent Tetraspeck beads 0.1 µm, 2×10^{15} particles / mL	Invitrogen	Cat# T7279
Triton X-100	Sigma-Aldrich	Cat# T9284
Sodium tetraborate decahydrate (Borax)	Sigma-Aldrich	Cat# B9876
Boric acid	Sigma-Aldrich	Cat# B6768
HBSS	Thermo Fisher Scientific	Cat# 14025050
GlutaMAX	Thermo Fisher Scientific	Cat# 35050038
Penicillin-streptomycin	Thermo Fisher Scientific	Cat# 15140122
Cytosine β-D-arabinofuranoside (Ara-C)	Sigma-Aldrich	Cat# C6645
Acridine orange/propidium iodide stain	Logos	Cat# F23001

(*Continued on next page*)

Continued		
REAGENT or RESOURCE	SOURCE	IDENTIFIER
Critical commercial assays		
P3 primary cell 4D-Nucleofactor X kit L	Lonza	Cat# V4XP-3024
Experimental models: Organisms/strains		
Pregnant adult Sprague-Dawley rat females	Janvier Labs	RjHan:SD
Recombinant DNA		
Plasmid: Xph20-mEos3.2	M. Sainlos (Rimbault et al.; Rimbault et al.)[4,5]	N/A
Plasmid: GFP-actin	A. Matus (Fischer et al.)[3]	N/A
Plasmid: mEos3.2-actin	Garcia et al.[6]	N/A
Software and algorithms		
FIJI	Schneider et al.[8]	http://fiji.sc
ThunderSTORM	Ovesný et al.[9]	RRID:SCR_016897; https://github.com/zitmen/thunderstorm
MetaMorph 64-bits v7.10	Molecular Devices	RRID:SCR_002368; http://www.moleculardevices.com/Products/Software/Meta-Imaging-Series/MetaMorph.html
SR-Tesseler v1.0	Levet et al.[10]	https://github.com/flevet/SR-Tesseler/releases/tag/v1.0
PoCA v0.10.0	Levet et al.[11]	https://github.com/flevet/PoCA https://doi.org/10.5281/zenodo.10112543
PALMTracer v2.0	Izeddin et al.[12,13]	https://goo.gl/forms/kGAgVUrnWzoEFivW2
Python	Python Software Foundation	RRID:SCR_008394; https://www.python.org
Napari	Napari	RRID:SCR_022765; https://napari.org
Napari-bead-reg v1.0	F. Levet, this paper	https://github.com/flevet/napari-beadreg https://doi.org/10.5281/zenodo.11197887
Other		
0.22 µm filtration unit ClearLine	Dutscher	Cat# 051732
Tissue culture dish easy-grip 35 × 10 mm Falcon	Dutscher	Cat# 353001
Tissue culture dish easy-grip 60 × 15 mm Falcon	Dutscher	Cat# 353004
Petri dish 92 × 16 mm	Sarstedt	Cat# 82.1473
6-well tissue culture plate Falcon	Dutscher	Cat# 353046
Photoetched coverslips 18 × 18 mm	Electron Microscopy Sciences	Cat# 72264-18
Cell counter LUNA-FL	Logos Biosystems	https://logosbio.com/luna-fl/
Inox Ludin chamber square 18 × 18 mm	Life Imaging Services	N/A
PALM microscope	Nikon ECLIPSE TiE	https://www.microscope.healthcare.nikon.com/fr_EU/products/inverted-microscopes/eclipse-ti-series
STED microscope	Leica SP8 WLL2	https://www.bic.u-bordeaux.fr/equipment/microscope-confocal-sp8-sted/

MATERIALS AND EQUIPMENT

- Buffers. Ara-C stock solution (1 mM): dilute 10 mg Ara-C powder in 42 mL H_2O. Sterile-filter the solution at 0.22 µm, aliquot, and store at −20°C for up to 3 months.

Feeding medium		
Reagent	Final concentration	Amount
GlutaMAX	0.5 mM	1.25 mL
B27 Plus 50×	1×	10 mL
Neurobasal Plus	N/A	490 mL
The final solution must be stored at 4°C for up to 1 month.		

Dissection buffer		
Reagent	Final concentration	Amount
HEPES buffer 1 M	7 mM	3.5 mL
Penicillin-Streptomycin 100×	1%	5 mL
HBSS	N/A	500 mL
The final solution must be stored at 4°C for up to 1 month.		

Trypsin solution		
Reagent	Final concentration	Amount
Penicillin-Streptomycin 100×	1%	1 mL
HEPES buffer 1 M	10 mM	1 mL
Trypsin-EDTA	N/A	100 mL
The final solution must be stored at 4°C for up to 6 months.		

Plating medium		
Reagent	Final concentration	Amount
GlutaMAX	1%	5 mL
Horse serum	10%	50 mL
DMEM	N/A	450 mL
The final solution must be stored at 4°C for up to 1 month.		

Borate buffer		
Reagent	Final concentration	Amount
Borax	12.5 mM	3.8 g
Boric Acid	50 mM	2.48 g
H_2O	N/A	800 mL
pH must be adjusted to 8.3 by adding HCl. The final solution must be stored at 4°C for up to 1 month.		

Tyrode solution		
Reagent	Final concentration	Amount
NaCl	108 mM	6.31 g
KCl	5 mM	372 mg
$MgCl_2$ $(H_20)_6$	2 mM	410 mg
$CaCl_2(H_20)_2$	2 mM	294 mg
D-Glucose	15 mM	2.703 g
HEPES powder	25 mM	5.97 g
H_2O	N/A	1 L
pH must be adjusted to 7.4 by adding drops of a 10 M NaOH solution; check that the osmolarity is around 280 mOsm; the final solution must be filtered under sterile conditions and can be stored at 4°C for up to 6 months.		

PFA – sucrose solution 4×		
Reagent	Final concentration	Amount
Paraformaldehyde	16%	32 g
Sucrose	16%	32 g
PBS	1×	200 mL
H_2O	N/A	100 mL
pH must be adjusted to 7.4 by adding HCl. The final solution is aliquoted in volumes of 3 mL in 15 mL tubes and stored at −20°C.		

- Fixation solution: dilute 3 mL of 4× PFA-sucrose solution in 9 mL Phosphate Buffered Saline (PBS).

Should be preferably prepared fresh but can be stored up to 1 week at 4°C.

⚠ CRITICAL: Manipulation of PFA is dangerous. Preparation must be done under a chemical fume hood, wearing appropriate protective equipment.

NH_4Cl solution		
Reagent	Final concentration	Amount
NH_4Cl	50 mM	1.34 g
PBS 10×	1×	50 mL
H_2O	N/A	450 mL
Can be stored at 22°C for several weeks on the shelf.		

- Permeabilization solution at 0.1%: add 1 mL of 1% Triton X-100 to 9 mL PBS.

Can be kept up to one week at 22°C.

- Blocking solution: 1% BSA in PBS (add 100 mg BSA to 10 mL PBS).

Should be prepared fresh and cannot be kept thereafter.

- STED observation medium: 50% glycerol, 50% PBS.

Storage at 22°C.

- **PALM set-up.**

The PALM set-up is based on a fully motorized Nikon Ti-Eclipse microscope (Nikon France S.A.S., Champigny-sur-Marne, France) equipped with a Perfect Focus System (PFS) to avoid axial drift, a 2D stage TI-S-ER, a metal halide lamp for epifluorescence (Nikon Xcite), and a Total Internal Reflection Fluorescence (TIRF) arm connected to an optical fiber fed by a 4-color laser bench containing 405 nm, 491 nm, and 561 nm diodes (all 100 mW nominal power).[6,14] Laser power is controlled through a multi-channel acousto-optical tunable filter (AOTF). Images are acquired using a 20× dry NA 0.5 Plan Fluor objective (to track the cells relative to etched patterns) and a 100× NA 1.49 ApoTIRF oil immersion objective (to perform PALM acquisitions). Appropriate interferential filters (Semrock, Rochester, NY, USA) are placed in excitation and emission filter wheels (Sutter Instruments, Novato, CA, USA). For GFP, we use a FF02 472/30 excitation filter, a FF01 495Di03 dichroic mirror, and a FF01 520/35 emission filter. For mEos3.2 photoconversion, both the 405 nm and the 561 nm lasers are projected to the sample via a Di02-R561 dichroic mirror and the emitted fluorescence is collected through a FF01 676/29 nm emission filter. For each center quadrant region of 256 × 256 pixels, image stacks are acquired in stream mode with an Evolve EMCCD camera of pixel size 16 μm (Photometrics, Tucson, USA). The whole system is controlled by MetaMorph (Molecular Devices, Sunnyvale, USA).

- **PALMTracer software.**

The image stacks obtained in PALM were analyzed using the PALMTracer software, a MetaMorph add-on.[12,13,15] Single molecule localization was achieved using wavelet segmentation, then filtered out based on the quality of a 2D Gaussian fit. PALMTracer generates a unique point cloud representing all the localizations coordinates. By setting a user-defined pixel size (i.e., the actual camera pixel

size divided by an adjustable scaling factor), this cloud can subsequently be used to create super-resolved images by per-pixel summation of the intensities of all localized single molecules (i.e., 1 detection per frame is coded by an intensity value of 1). The choice of the scaling factor (typically 5) aims at reaching a final pixel size (32 nm) on the reconstructed image compatible with the expected resolution of the technique.

- **ThunderSTORM software.**

The image stacks obtained in PALM were also analyzed using ThunderSTORM,[9] an ImageJ[8] plugin. Raw images were first pretreated using a wavelet filter to improve events detections using a local maxima algorithm. The detected objects were then fitted using a 2D Gaussian function to obtain file giving the subpixel localizations of all molecules. From this localization file, a unique super-resolved image with an adjustable scaling factor can also be reconstructed.

- **STED microscope.**

The confocal STED microscope is a Leica SP8 WLL2 plugged on an inverted stand DMI6000 (Leica Microsystems, Mannheim, Germany). Images were acquired using a 20× multi-immersion NA 0.75 HC Plan Apo CS2 objective and a 93× Glycerol NA 1.3 HC PL APO CS2 motCORR objective, and the pinhole was set at 1 times the Airy disk. The microscope is equipped with a white light laser 2 (WLL2) with freely tunable excitation from 470 to 670 nm (1 nm steps). Scanning was done using a conventional scanner running at a frequency of 400 Hz, and an image format of 1280 × 1280 pixels was chosen. The zoom factor was adjusted to reach a pixel size of either 160 nm or 32 nm, so as to fit the format of images acquired in PALM at low or high resolution, respectively. An internal hybrid detector was used for the acquisition of fluorescence signals, and an external photomultiplier tube (PMT) was used for transmission. For confocal acquisition, the WLL2 was set at 488 nm to image GFP, at 561 nm to image Tetraspeck beads, and at 640 nm to image Atto647N. For STED acquisition, depletion of Atto647N dyes was performed in 2D using the 775 nm wavelength.

- **Napari-beadreg.**

Alignment of the STED images and SMLM localizations was done with napari-beadreg, a custom made napari plugin that computes a non-linear transformation using beads as landmarks. Napari-beadreg requires therefore to load the beads positions from each of the microscopy modalities, with the SMLM and STED beads being the source and target landmarks, respectively. Upon loading, our plugin automatically links each bead of one modality to the nearest neighbor bead of the other modality. For simplicity, a graph representation is created with Networkx (https://networkx.org/), with its nodes being the complete set of beads and its edges the links between beads of the two modalities. Erroneously connected beads can be easily corrected by adding or removing edges from the graph with mouse clicks. Then, thin plate splines[16] are used to compute a non-rigid (warping) transformation moving the source landmarks to the exact positions of the target landmarks they are connected to. Finally, this transformation is applied to each localization of the SMLM dataset, and the transformed localizations are saved for further correlative analysis with the STED images.

- **SR-Tesseler.**

Identification and measurements of the number and size of PSD-95 nanodomains were achieved using SR-Tesseler, an object segmentation approach based on Voronoï tessellation[10] constructed from the coordinates of the single molecules previously obtained using PALMTracer.

STEP-BY-STEP METHOD DETAILS

Cell fixation

Timing: 1 h

This section describes how to fix cell cultures prior to imaging. Although PALM and STED experiments can both be performed live,[1,17] the facts that we need to change microscopes between the two imaging modalities and amplify the GFP-actin signal by immunocytochemistry for STED make it necessary to fix the samples.

1. Fill as many wells of a 6-well tissue culture plate with 2 mL of Tyrode solution pre-warmed at 37°C, as there are coverslips to treat.
2. Take the dishes containing each 2 etched coverslips of previously electroporated neurons (before you begin, Step 11e), now at DIV 14.
3. Place each coverslip upside down into separate wells of the 6-well plate, and leave them there for less than 2 min.

Note: Do not forget that neurons have been cultured face down onto the glial cell feeder layer, so that coverslips now have to be flipped by 180° for neurons to face up.

⚠ CRITICAL: At this step, as the neurons are alive, one has to be very careful that the Tyrode solution is at 37°C, and time to fixation has to be kept as short as possible.

4. Remove the Tyrode solution off each well containing a coverslip and add 2 mL of warm Tyrode solution. Leave them for less than 2 min.

⚠ CRITICAL: PFA manipulation must be done under a chemical hood wearing gloves and a lab coat. PFA must be disposed of in a special container for proper elimination.

5. Under a chemical hood,
   a. Remove the Tyrode solution.
   b. Add 2 mL of fixation solution to each well containing a coverslip.
   c. Incubate for 10 min at 22°C.
6. Wash 3 times for 1 min with 2 mL of PBS.

⚠ CRITICAL: The fixation solution and the first PBS wash should be eliminated in the appropriate waste container.

7. Outside the chemical hood,
   a. Remove PBS.
   b. Add 2 mL of NH_4Cl solution to each well containing a coverslip.
   c. Incubate for 15 min.

Note: This step aims at blocking free aldehydes to avoid non-specific labeling.

8. Wash 3 times with 2 mL PBS and keep the cells at 4°C until ready for PALM acquisition.

Pause point: After fixation, coverslips can be stored at 4°C for a few days, but it is recommended to proceed to the PALM acquisition as soon as possible to avoid sample contamination.

Acquisition of PALM data

Timing: 4 h, for a typical number of 5 PALM acquisitions

This section describes the steps to acquire PALM data from single neurons. It comprises the procedures to introduce Tetraspeck beads on coverslips to eventually correct for microscope drift, localize neurons of interest based on the GFP-actin signal, and memorize their positions thanks to etched coverslips. Recorded positions will be used to track the same cells later in STED microscopy. PALM itself generates image stacks of single photoconverted Xph20-mEos3.2 molecules that label the synaptic protein PSD-95, together with positions of fiducial beads.

9. Mix 4 μL of tetraspeck beads with 1 mL of PBS in a 1.5 mL conical tube to obtain a final solution at 0.4%.

   Note: This represents a concentration of 8.0×10^{12} particles /mL. In the end, we aim at having around 10–20 beads stuck to the coverslip per field of view (1677 μm^2).

   ⚠ CRITICAL: Tetraspeck beads tend to stick to the tube wall, thus the bead dilution should be used within hours of preparation and not kept thereafter.

10. Place coverslips on a piece of Parafilm with cells facing up.
    a. Add 300 μL of the diluted solution of Tetraspeck beads on the coverslip.
    b. Incubate for 5 min.

    Note: This strategy is used to minimize the volume of Tetraspeck beads put on the coverslip.

11. Place the coverslip back to the 6 well plate, wash one time with 2 mL PBS, and proceed with PALM acquisition.

    Note: The beads will stick to the coverslip and be used for 2 different processes: i) the correction of the potential microscope drift upon reconstruction of the PALM super-resolved image; and ii) the registration of the images acquired in both PALM and STED modes.

12. Place an etched coverslip containing the previously fixed neurons in a suitable imaging chamber that allows coverslips to be easily mounted and dismounted (here a square 18 × 18 mm Inox Ludin chamber (Life Imaging Services, GmbH, Basel, Switzerland). Fill the chamber with 1 mL PBS and place it on the PALM set-up (Figure 2A).
13. First use the 20× objective and DIC illumination to locate the letters and numbers on the etched coverslip and potentially turn the chamber to obtain the straight orientation of the patterns.
14. Change to the 100× objective. Use the GFP-actin channel to find a neuron of interest and move the 2D stage to center the region of interest (ROI) in the field of view of the camera that will be acquired (here the center quadrant of 256 × 256 pixels) (Figure 2B).
15. PALM acquisition.
    a. Switch to the mEos3.2 illumination setting.
    b. Increase the input power of the 561 nm laser line to visualize already photoconverted mEos3.2 proteins.

    Note: We typically use 30%–40% of the 100 mW 561 nm laser, corresponding to 5–7 mW at the objective front lens (there is power loss in the optical fiber and the microscope optics). Under these conditions, the lifetime of individual mEos3.2 molecules before photobleaching is around 300 ms.

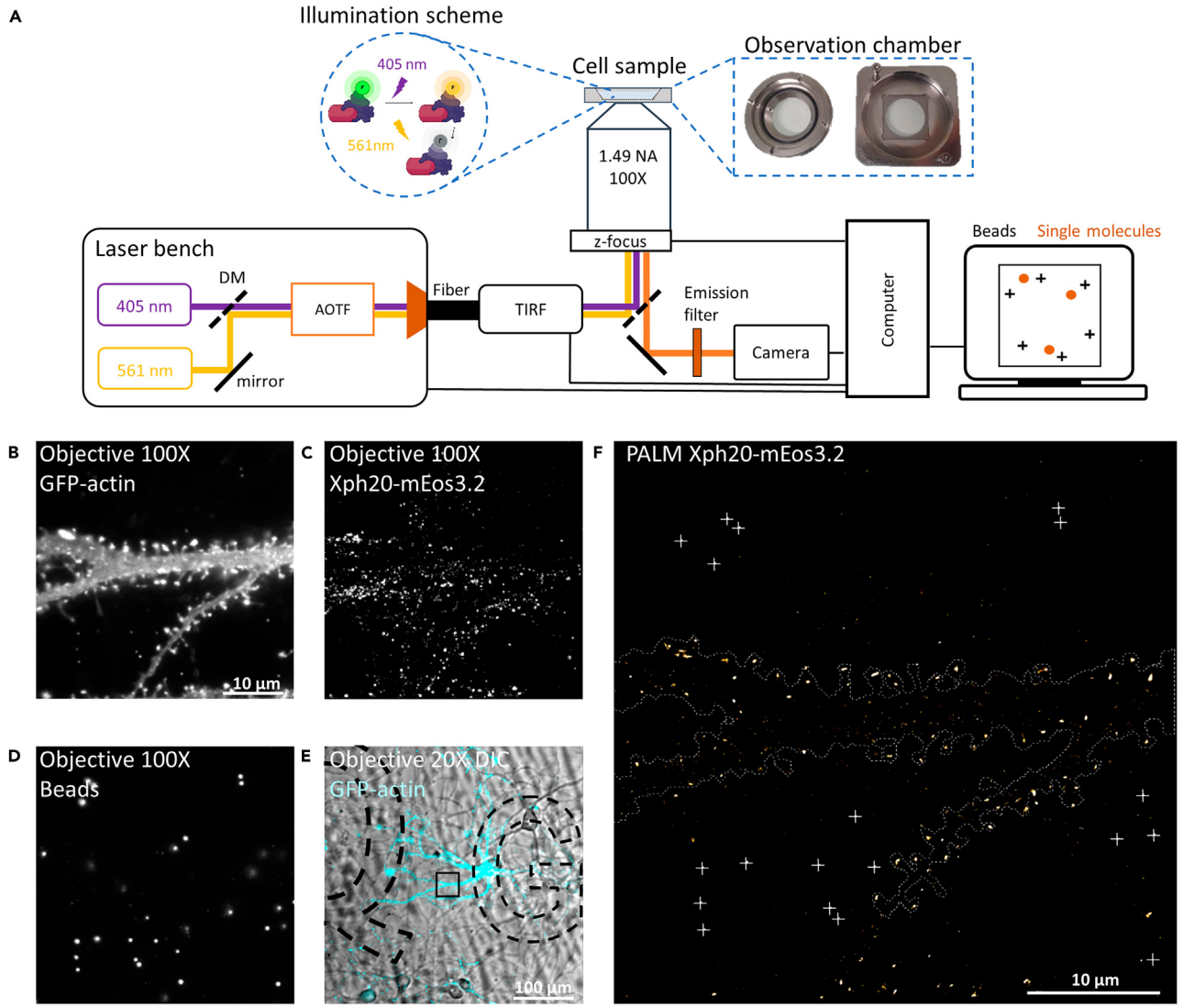

Figure 2. PALM acquisition of PSD-95 based on the Xph20-mEos3.2 intrabody

(A) Schematic diagram of the PALM setup. DM: dichroic mirror; TIRF: Total internal reflection fluorescence; AOTF: acousto-optic tunable filter.

(B) Image of the dendritic tree of a neuron expressing GFP-actin, taken with the 100× objective under 491 nm illumination.

(C and D) Images of the same field of view acquired at 561 nm. (C) Subtraction between the maximum projection image and the average image of the fluorescence signal integrated over 2'000 frames, highlighting the localizations of the Xph20-mEos3.2 molecules over the signal from the 100-nm Tetraspeck beads. (D) Single frame image revealing essentially the localizations of the beads, which are much brighter than single molecules. The format of images B-D is 256 × 256 pixels (pixel size 160 nm).

(E) Bright field image of the same area taken with the 20× objective, onto which the image of the GFP-actin positive neuron was superimposed in cyan.

(F) Super-resolved image of PSD-95 integrating all detections from the single Xph20-mEos3.2 molecules (pixel size 32 nm, zoom 5 with respect to the original images). White crosses represent the positions of the beads localized in single pixels.

c. Gradually increase the 405 nm laser intensity (typically 5–15% of the 50 mW nominal power, corresponding to 3–6 µW at the objective front lens), to induce mEos3.2 photo-conversion from the green-emitting to the red-emitting form.

Note: A steady-state is quickly reached where mEos3.2 photoconversion induced by the 405 nm laser compensates for mEos3.2 photobleaching through the 561 nm laser, and a relatively stable number of molecules are detected per frame. In these conditions, we aim at

visualizing between 50 and 200 well-separated molecules per field of view, depending on the expression level of the protein of interest.

d. Finally, tune the TIRF illumination angle and the focus to visually optimize the signal-to-noise ratio.

Note: This parameter depends on the microscope objective, the laser intensity, the TIRF angle, and the type of camera used (e.g. EMCCD vs sCMOS). A typical value in our conditions is 2.2 for mEos3.2 and 9.1 for Tetraspeck beads.

⚠ CRITICAL: At this step, different parameters can be modulated to obtain a good detection of single emission events. One can tune laser intensities (405 nm and 561 nm), the illumination angle, and the focus. This fine tuning is critical as the quality of the final image based on the precision of the localization of each individual event depends on the number of photons detected per molecule and per frame.

e. Acquire a stream of 2,000 frames at a 50 Hz frequency, i.e., with an exposure time of 20 ms (Methods video S1). From this raw stack, generate a maximum image where the mEos3.2 molecules are seen to fill the dendritic contour (Figure 2C), as well as an average image which shows essentially the Tetraspeck beads appearing as very bright spots compared to the single mEos3.2 proteins (Figure 2D).

Note: If the mEos3.2 signal is bright and persistent, one can accumulate more detections, by carrying out several cycles of stream acquisitions (typically 4–6, corresponding to 8000–12000 frames).

f. To detect all beads in the field of view, acquire a small z-stack of 5–10 images under the 561 nm illumination setting with a z-increment of 0.3 μm using the z-motor of the microscope, and generate a maximal projection image of this stack.

Note: Tetraspeck beads will be used later to correlate PALM and STED images in the Napari plugin. To do so, it is necessary to have at least 10 beads per field of view.

⚠ CRITICAL: For the next step, X and Y positions should not be changed to keep the exact same location of the cell in the field of view to be able to recover it later when switching to the STED microscope. The 2D stage can be moved after step 16.

16. Localize the neuron of interest.
    a. Set the 20× objective and acquire a full field image (here 512 × 512 pixels) of the GFP-actin channel (Figure 2E, cyan).
    b. Using DIC illumination, acquire a full field image of the neuron and the surrounding patterns (Figure 2E, gray).
    c. If the patterns are fuzzy, move the 2D stage to find the closest grid indications with a clear combination of numbers and letters, to make sure of the X,Y position of the recorded neuron.
17. Repeat the PALM procedure as many times as required to image a sufficient number of cells per coverslip (typically up to 5).
18. After all PALM acquisitions are done, place the coverslip (cells facing up) back into a 6-well plate containing PBS at 4°C.

Note: The procedure to reconstruct the final super-resolved image (Figure 2F) will be explained in Step 29.

Pause point: After PALM acquisitions, fixed coverslips can be stored at 4°C for a few days, but it is recommended to proceed to the immunolabeling steps as soon as possible to avoid sample contamination with bacteria or fungi.

Immunocytochemistry

Timing: 4 h

Because STED microscopy requires bright fluorescent signals to compensate for the depletion effect, immunocytochemistry is necessary to amplify the rather low signals from fluorescent proteins such as GFP. This section describes the immunofluorescence labeling of actin-GFP with a robust chemical fluorophore adapted to STED acquisition (here Atto-647N). This procedure is applied to the same coverslips previously imaged with PALM.

19. Permeabilization step.
    a. Remove the PBS.
    b. Add 2 mL of permeabilization solution to as many wells of the 6-well culture plate as there are coverslips.
    c. Incubate for 5 min on the shelf.
    d. Remove the permeabilization solution.
    e. Wash the coverslips 3 times with PBS for 5 min.

Note: Washing coverslips with PBS can detach the cells, thus proceed carefully.

20. Blocking step.
    a. Remove the PBS.
    b. Fill the wells with 2 mL of blocking solution.
    c. Incubate for 30 min.
21. Primary antibody incubation.
    a. Prepare the primary antibody dilution in the blocking solution.

Note: Here, mouse anti-GFP is used at 1:1000.

    b. Add 300 μL of primary antibody solution on a piece of Parafilm.
    c. Flip the etched coverslip onto the drop.
    d. Incubate for 1 h at 22°C in a dark environment.

Note: The paraffin dots act as spacers and the drop spreads below the entire coverslip. This arrangement is designed to use a minimum amount of antibody.

22. Washing step.
    a. Flip the coverslips back into the 6-well plate containing blocking solution.
    b. Wash 3 times 5 min with blocking solution.
23. Secondary antibody incubation. Repeat step 21 with secondary antibodies.

Note: Here, goat anti- mouse Atto-647N was diluted at 1:500. Antibody dilutions should be adjusted on a per user basis, depending on the antibody source and protein expression levels (See troubleshooting problem 3).

24. Finally wash 3 times with 2 mL of PBS.

Table 1. Correspondence between PALM and STED acquisition parameters, related to steps 28 and 33

PALM

Parameters	ROI	Camera pixel size	Objective magnification	Scaling factor	Image format	Pixel size	Field of view
Unit	pixels	µm	–	–	pixels	nm	µm
	256	16	100	5	1280	32	40.96
	360	13	100	4	1440	32.5	46.8
	400	11	100	3	1200	36.67	44

STED

Parameters	Laser scanning field	Objective magnification	Optical zoom	Image format	Pixel size	Field of view
Unit	zoom x1 (µm)	–	–	pixels	nm	µm
	125	93	3.05	1280	32	40.98
	125	93	2.67	1440	32.5	46.82
	125	93	2.83	1200	36.67	44.17

Three different examples of ROI size, camera pixel size, and digital scaling factors are chosen for PALM (conditions 1, 2, and 3), and the STED acquisition parameters are adjusted in each condition to eventually reach the same image size in both imaging modes. Using a fixed laser scanning field determined by the set-up, the optical zoom in STED is set to match the field of view imaged in PALM, taking into account a potential difference in objective magnification. Finally, the image format in STED is set equal to the super-resolved image in PALM, which depends on the ROI and digital zoom. This ensures that the final pixel size of super-resolved PALM and STED images is the same (around 30 nm).

Pause point: After immunolabeling, fixed coverslips can be stored at 4°C for several hours, but it is recommended to proceed to the STED acquisition as soon as possible to avoid diffusion of the staining and fading of the fluorescence.

STED acquisition

Timing: 3 h

This section describes the use of STED microscopy to obtain the morphology of the dendrites from neurons previously imaged by PALM, and based on the GFP-actin signal amplified by immunolabeling with Atto-647N-conjugated antibodies.

⚠ CRITICAL: At this stage, it is critical to acquire STED images with the same properties as the super-resolved PALM image (same field of view, image format, and pixel size). Here the values given are based on the specifications of the two microscopes we used for this study. To reproduce this protocol, one should adapt the optical zoom and format in STED based on the specificities of PALM acquisitions. A set of corresponding parameters is given in Table 1.

25. Mount the coverslip in the square Ludin chamber, add 1 mL of STED observation medium, and place on the STED microscope (Figure 3A).
26. Locate a neuron of interest.
    a. Set the 20× objective.
    b. Using eyepieces and transmitted light, locate the region on the etched coverslip corresponding to the area previously acquired in PALM.
    c. Using the transmitted light and 647 nm excitation in confocal mode, center the neuronal region to image by finely moving the 2D stage.
    d. Using a low zoom factor e.g., 1.4, acquire 2 reference images of 1280 × 1280 pixels showing the etched pattern (Figure 3B) and the GFP-actin signal amplified with Atto-647N conjugated antibodies (Figure 3C).
27. Confocal acquisitions.
    a. Change the objective from 20× to 93× (objective dedicated to STED) without moving the X and Y positions.

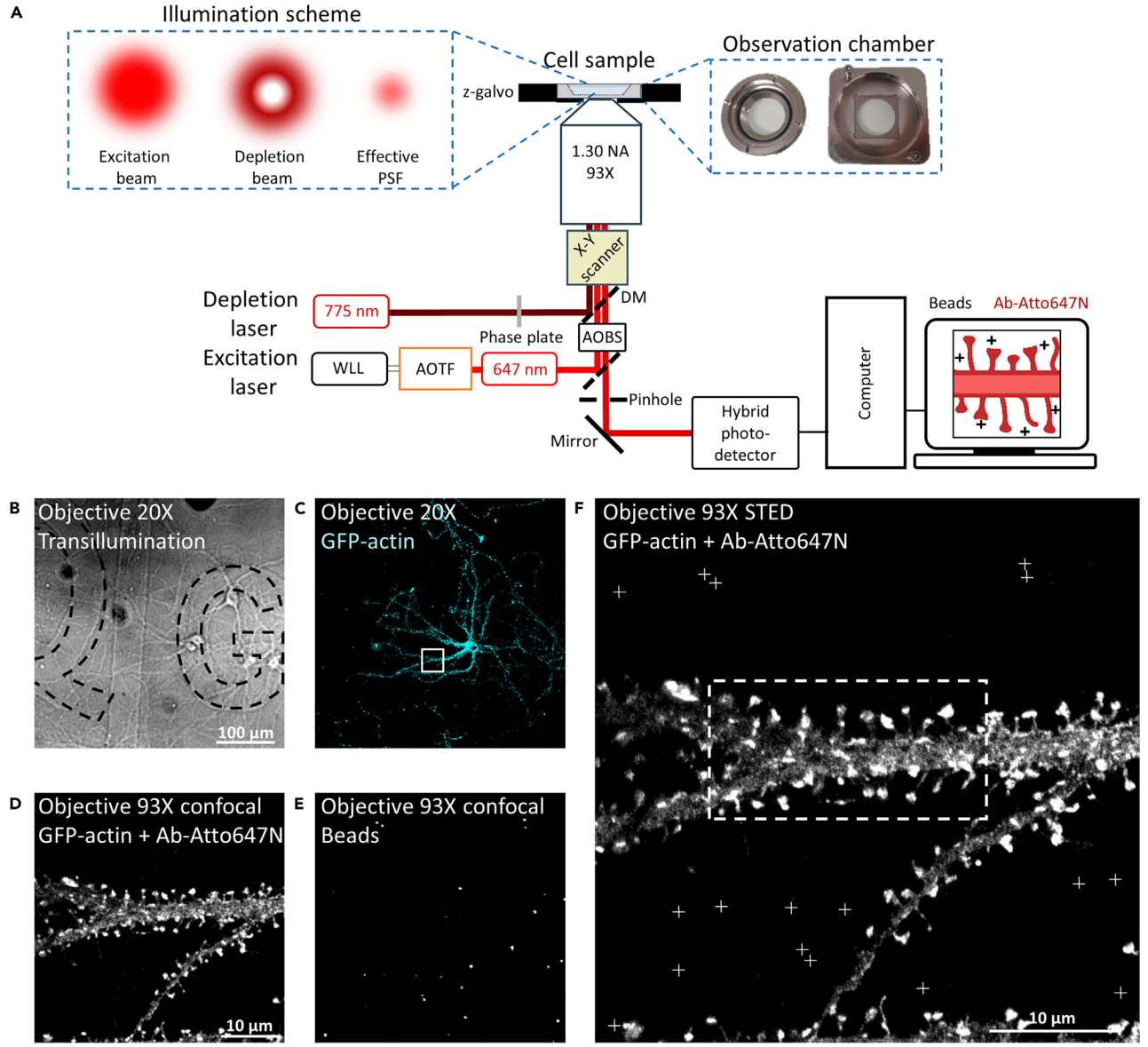

Figure 3. STED acquisition of immunolabeled GFP-actin

(A) Schematic diagram of the STED set-up. WLL: white light laser; AOTF: acousto-optic tunable filter; AOBS: Acousto-optical beam splitter.

(B) Transmission confocal image of the same area selected in Figure 2, identified by the QG pattern with a 20× objective.

(C) Corresponding image of the GFP-actin signal, which is highlighted in cyan.

(D) Confocal image taken with the 93× objective in the Atto-647N channel where the laser beam scans the central square area highlighted in C (1280 × 1280 pixels).

(E) Corresponding confocal image of the Tetraspeck beads in the red channel (570–620 nm window).

(F) STED image of GFP-actin immuno-labeled with anti-GFP primary and Atto-647N-conjugated secondary antibodies (Ab-Atto647N). The dashed rectangle area will be further zoomed in Figure 6D.

b. Set the zoom to reach a pixel size of 32 nm.

c. Acquire an image of the neuron of interest in confocal mode (excitation wavelength at 647 nm, detection window between 654-707 nm, image format 1280 pixels × 1280 pixels), based on the Atto-647N signal (Figure 3D).

d. Using 561 nm illumination, locate the beads in the field of view.

e. If necessary, using the precise motion of the 2D-stage, finely adjust the field position using the PALM bead image as a guide.

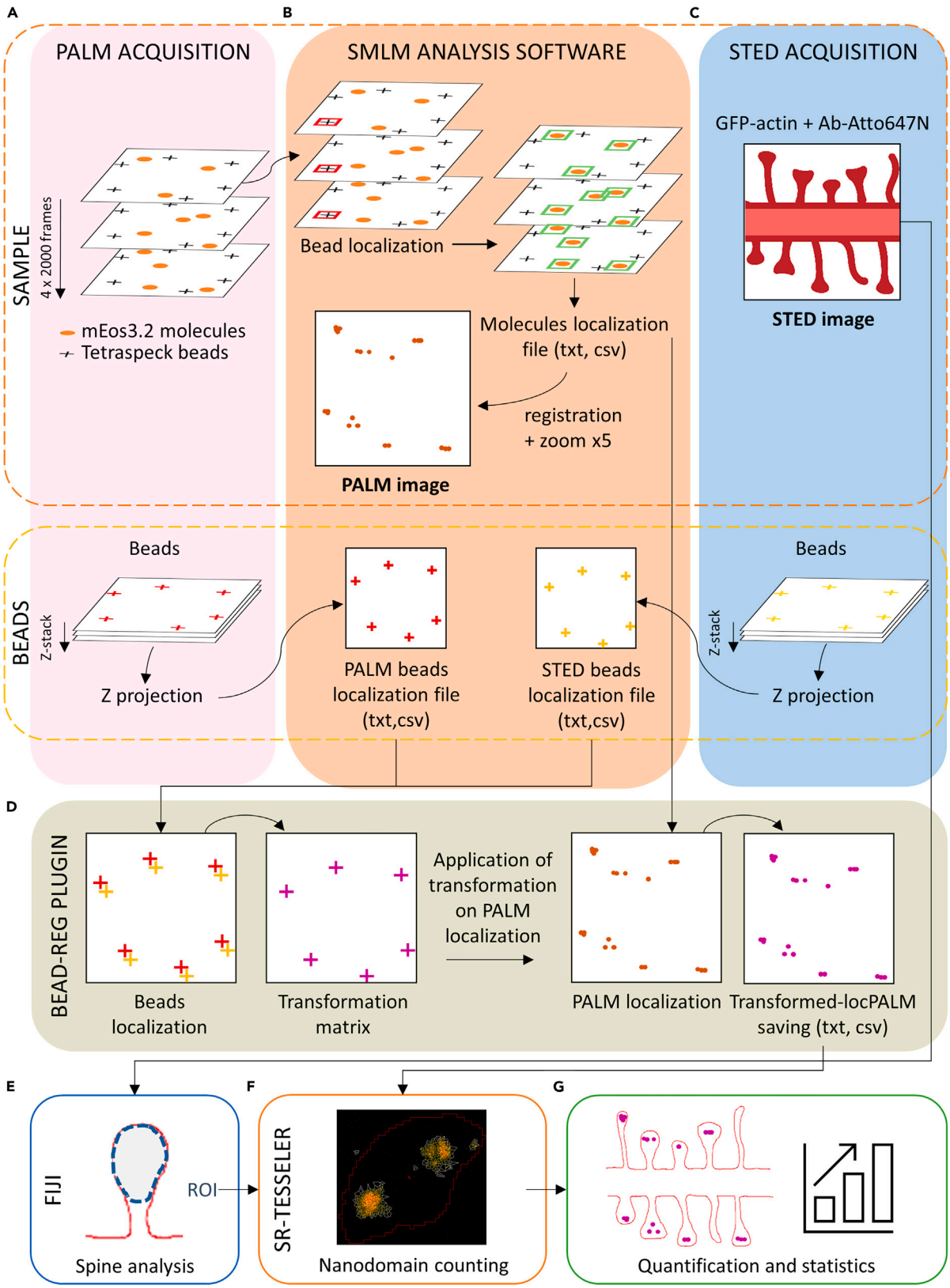
A
B
C
PALM ACQUISITION
SMLM ANALYSIS SOFTWARE
STED ACQUISITION
SAMPLE
4 x 2000 frames
mEos3.2 molecules
Tetraspeck beads
Bead localization
Molecules localization file (txt, csv)
registration + zoom x5
PALM image
GFP-actin + Ab-Atto647N
STED image
BEADS
Beads
Z-stack
Z projection
PALM beads localization file (txt,csv)
STED beads localization file (txt,csv)
Beads
Z-stack
Z projection
D
BEAD-REG PLUGIN
Beads localization
Transformation matrix
Application of transformation on PALM localization
PALM localization
Transformed-locPALM saving (txt, csv)
E
F
G
FIJI
ROI
Spine analysis
SR-TESSELER
Nanodomain counting
Quantification and statistics

Figure 4. Image analysis pipeline

(A) PALM acquisitions consist of 4–6 temporal streams of 2,000 images each, containing the fluorescence signals from both mEos3.2 fusion proteins and Tetraspeck beads.

(B) Image stacks are then opened in SMLM software such as PALMTracer or ThunderSTORM. By setting a high detection threshold, one bead is chosen to correct for lateral drift. Then, by setting a lower detection threshold, single mEos3.2 molecules are detected, and a localization file is created, after applying the drift correction to all molecules. A single super-resolved image is created with a zoom factor of 5 (PALM image).

(C) STED acquisitions give a single image from the Atto647N signal recognizing GFP-actin by immunocytochemistry (Ab-Atto647N). Because of potential depth in the sample, not all beads emit homogeneously. Thus, a small 3D stack is acquired in both TIRF and confocal modes (PALM and STED panels, respectively) and a maximal intensity projection is created to image all the beads equivalently. The SMLM software is used to create two separate localization files from the bead projection images obtained in PALM and STED, respectively.

(D) Those files are then opened in Napari-bead-reg to create an image transformation matrix, which is applied to the single mEos3.2 molecule localization file, creating a transformed localization file. A new PALM image can then be generated with the SMLM software and super-imposed to the STED image.

(E) FIJI is used to segment dendritic spines from STED images and calculate their projected area. The ROI drawn for each spine is exported to SR-Tesseler.

(F) The SR-Tesseler software is then used to highlight the nanodomains formed in PALM images by some proteins such as PSD-95, count their number per spine, and measure their size.

(G) Finally, the data are computed for a few dual PALM-STED acquisitions on individual neurons, and statistics are made.

f. For later image correlation, acquire a z-stack (5–10 planes with a 0.3 µm z increment) of the Tetraspeck beads using 561 nm illumination (Figure 3E). To fit the corresponding low resolution image previously acquired in PALM mode, change the format to 256 × 256 pixels. This stack will be processed later in the Napari Plugin.

28. STED acquisition.
    a. Set back the image format to 1280 × 1280 pixels.
    b. Keep the zoom factor to 3.05 (final pixel size of 32 nm).
    c. Set the illumination parameters (excitation wavelength 647 nm, depletion wavelength 775 nm, detection window 654–707 nm, gating window 0.5–6 ns, 4 accumulations) to optimize the STED acquisition.
    d. Acquire a single STED image (Figure 3F).

Pause point: The experimental part is finished. The PALM image reconstruction and the PALM-STED image correlation can be done later at will.

Generating single molecule localization maps from PALM data

Timing: 1 h for a typical number of 5 super-resolved images

This section describes the successive steps to generate maps of single molecule localization data, spatially registered for any lateral drift that could have occurred during the acquisition, so as to reach the maximum lateral resolution for the reconstruction.

Note: Here the analysis process is described using PALMTracer[12] for detection, localization and drift correction. The full analysis process can also be achieved using other SMLM analysis freeware such as ThunderSTORM.[9] The acquired sequence contains two distinct signals: the relatively weak and blinking signal from individual mEos3.2 fusion proteins, and the bright and constant signal from the Tetraspeck beads (Figure 4A). Spatial registration is achieved using the Tetraspeck beads as fiducial markers, whose position on the sample is fixed and which can be detected on every image of the acquisition sequence. Beads can thus be tracked to measure the sample displacement due to mechanical drift. Then, on the same acquisition sequence, the detection and localization of single mEos3.2 molecules is performed. Finally, the displacement measured on the beads is applied to the localization list of the mEos3.2 fusion proteins to correct for the drift (Figure 4B). This two-step analysis allowed us to reconstruct the nanoscale map of the post-synaptic density protein PSD-95 or the cytoskeletal protein actin in dendritic segments.

29. Open the SMLM image processing software PALMTracer[12] to reconstruct the super-resolved image and get the list of localizations (Figure 4B).

Note: The detection of single events is done using wavelet segmentation and the precise sub-pixel localization is then performed by applying a Gaussian fit to the detected molecules. The user has to set a detection threshold to separate specific events from the background. The definition of this threshold is visually controlled thanks to a preview tool which applies a region around each detection, on the raw image sequence. One can then dynamically change the threshold and observe over the sequence the molecules that are detected. Once the threshold is set, the detection and fitting algorithm are launched to generate the localization list. The process can be divided in 4 sub-steps:

30. Detection of the beads.
    a. Focus on the fiducial markers signal (here Tetraspeck beads) to obtain their localization and measure the potential drift over time.
    b. Select a detection threshold adapted to detect the beads on all images of the sequence.
    c. Apply the detection and localization algorithms.

Note: By using the specific registration function of the software, the displacement of the beads over time is measured throughout all images of the sequence. This information will be used later to correct the localization list of the protein of interest.

31. Detection of single mEos3.2 fusion molecules.
    a. To select those signals above the background, focus this time only on the mEos3.2 signal which is much lower than that of the Tetraspeck beads.
    b. Define a new detection threshold using the preview tool to find the best value to detect the specific signal.
    c. Once the proper threshold has been defined, apply the detection and localization algorithms to generate the localization list.

⚠ CRITICAL: The threshold for detection must be correctly set to ensure that as much signal as possible is detected, and to avoid false positive and false negative detections. This setting is essential to obtain a good super-resolved image with a high localization precision.

32. Drift correction.
    a. In PALMTracer, use the specific registration function that corrects the localization list obtained for mEos3.2 signal based on the drift measured on the fiducial markers (step 30c).
    b. You now have generated a new corrected localization list that will be used for the rest of the analysis process.
33. Reconstruction of super-resolved images. Apply a scaling factor so that the sub pixel localizations obtained can be represented and sampled properly on the new digital image (Figure 2F). In our conditions, starting with original images of 256 × 256 pixels of 160 nm each, we applied a scaling factor of 5 to get a reconstructed image of 1280 × 1280 pixels with a final pixel size of 32 nm, around half the localization precision of our PALM system (FWHM = 60 nm)[18] (Figure 5A).

Note: In this image, the intensity represents the number of individual detections per pixel recorded over the whole batch of images stacks (e.g. from 3 × 2,000 = 6,000 images). In practice, the total number of single molecule localizations computed over the whole image batch, divided by the surface area of the corresponding dendritic segment was 4647 ± 645 μm^{-2} for Xph20-mEos3.2 and 12042 ± 735 μm^{-2} for mEos3.2-actin (mean ± SEM, n = 5 neurons for each condition).

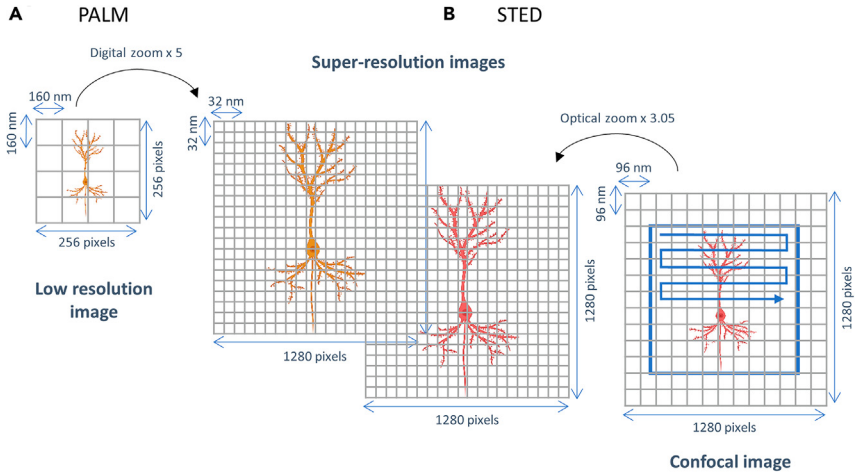

Figure 5. Correspondence between PALM and STED image formats

To correlate PALM and STED modes, we need to make a correspondence of the same field of view with images of the same format.

(A) PALM. The format of the low resolution image (256 × 256 pixels) is set by the size of the ROI with a uniform TIRF illumination (center quadrant in our case), the objective magnification (100×), and the pixel size of the camera (16 μm), resulting in an image pixel size of 160 nm and an actual field of view of 41 μm × 41 μm. To generate the super-resolved image (right), we apply a digital scaling factor of ×5, thereby creating an image of 1280 × 1280 pixels, each pixel being 32 nm in size. This format is then compatible with the 60 nm resolution offered by our PALM set-up.

(B) STED. To fit the PALM image, we choose the same image format (1280 × 1280 pixels) and set the optical scaling factor of 3.05 to obtain the same pixel size of 32 nm (left). The field of view scanned by the laser with the 93× objective now exactly corresponds to the ROI previously imaged by PALM.

Note: We have optimized the acquisition parameters on our microscopes and analysis software so as to produce super-resolved PALM and STED images of exactly the same format (Figure 5B). However, as these parameters may vary depending on the instruments, one has to adapt them accordingly. We provide in Table 1 a correspondence between PALM and STED imaging parameters for different combinations of ROI size and camera pixel size, the essential criterion being that the ROI imaged in PALM exactly corresponds to the region scanned by the laser in STED mode.

PALM-STED image correlation

Timing: 3 h

Although PALM and STED images now have the same format and pixel size, they still may show a little shift or rotation with respect to each other. This section describes how to precisely align the two images together, and thus optimally correlate both parameters of the study (nanoscale organization to sub-cellular volume). Here, the single molecule localizations obtained from PALM are projected onto the STED image.

34. Using either PALMTracer or ThunderSTORM, generate two localization files corresponding to the low resolution bead images acquired during PALM and STED acquisitions (steps 15f and 27f, respectively). As described in step 30b, set a high threshold to detect the beads (Figures 4A–4C).
35. Using the Napari-bead-reg plugin (Figure 4D),
    a. Load both the PALM and STED bead localization files previously generated (Figure 4B).

Note: The plugin automatically matches beads of the two modalities and tags potential aberrant links (Figure 6A). This tagging is performed in two steps. First, the median direction of all

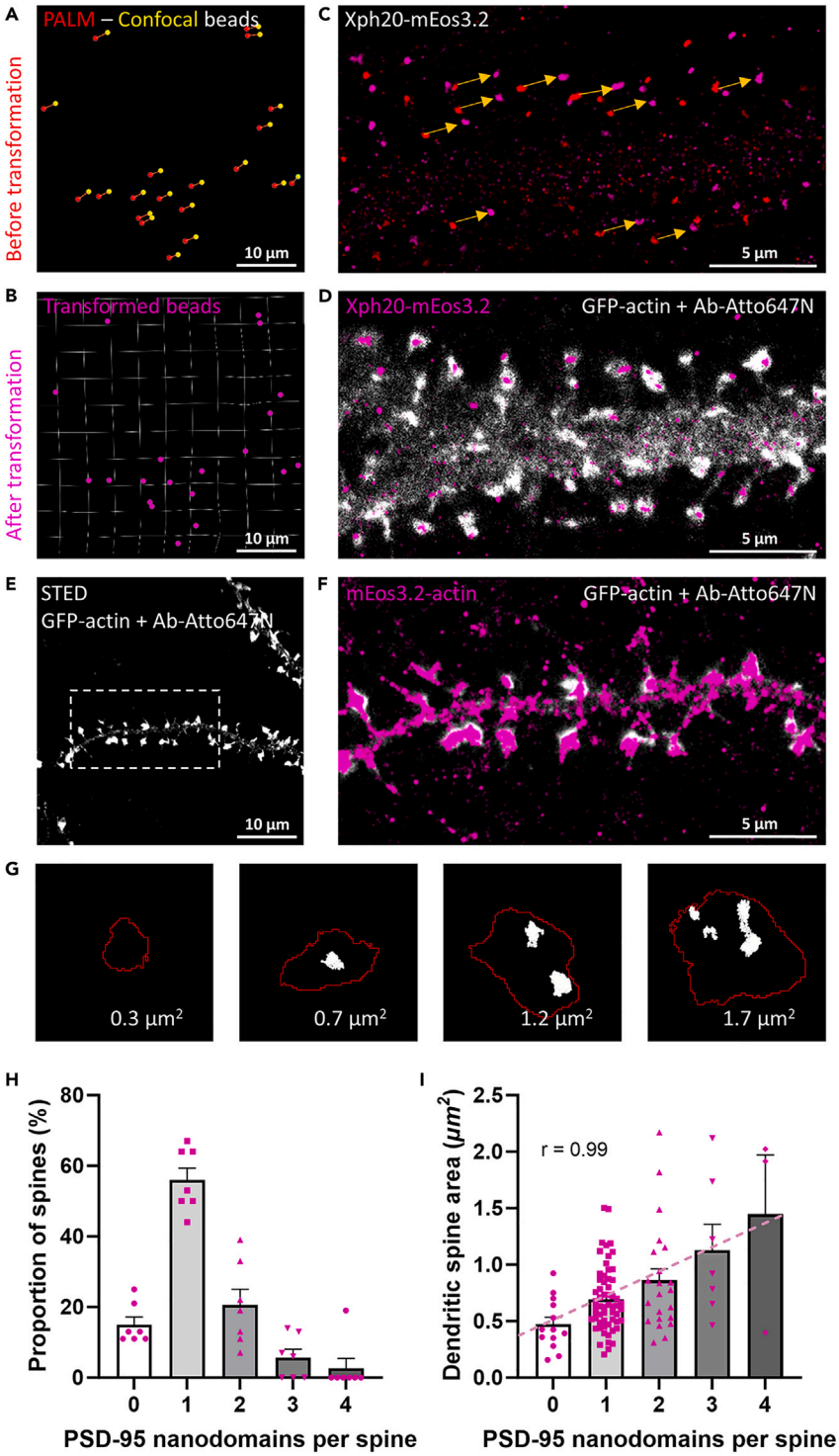

Figure 6. Correlation between PALM and STED images

(A) Merged image showing the localization of the Tetraspeck beads obtained from PALM and confocal channels (red and yellow, respectively). The centroids of each bead were determined with PALMTracer, imported in Napari, and represented here as circles. The lines show the connections made between the beads in the two channels, which served us to establish a transformation matrix converting the object localizations in PALM onto the confocal image. (B) Using this correspondence, the coordinates of the beads in PALM were transformed so as to align to the beads in the confocal image (now in magenta). The white grids display the local image deformations in the process.

Figure 6. *Continued*
(C) Zoom on a dendritic area from Figure 3F showing the reconstructed PALM images of the Xph20-mEos3.2 signal before (red) and after (magenta) transformation.
(D) Superimposition of the STED image of GFP-actin amplified with Atto647N conjugated antibody, Ab-Atto647N (white), with the transformed PALM image of PSD-95 labeled with the Xph20-mEos3.2 intrabody (magenta).
(E) Image of a neuron expressing GFP-actin amplified with Atto647N and imaged with STED.
(F) Correlative image between mEos3.2-actin (PALM) and GFP-actin signals (STED) of the dendritic segment delineated in (E).
(G) Representative images of individual dendritic spines containing 0, 1, 2, or 3 PSD-95 nanodomains (appearing in white). The spine contour is delineated in red and the corresponding projected area is indicated.
(H) Histogram showing the proportion of spines having 0, 1, 2, 3, or 4 nanodomains. Data are represented as mean ± SEM and dots represent individual neurons (n = 7).
(I) Bar graph showing the positive correlation between the number of PSD-95 nanodomains per spine, and the projected area of the whole spine. Data are represented as mean ± SEM and dots represent individual spines (n = 105 spines from 7 neurons).

the links is determined, and any link deviating more than 60 degrees from this direction is tagged as aberrant. Second, if a bead is connected to more than one bead in the other modality, the plugin only keeps the shortest link and tags all the remaining ones as aberrant.

b. Using the procedure explained above, manually add or remove any aberrant link, and finally delete them.
c. Create the image transformation based on the bead connections.

Note: Beads imaged in PALM (red) should now perfectly match the beads imaged in STED (yellow) (Figure 6B).

d. Load the localization file of the PALM acquisition and apply the transformation to the image of the neurons.

Note: One can now visualize the super-resolved single molecule PALM localization maps before (red) and after (magenta) the transformation (Figure 6C).

e. Save the transformed localization file which will be used later for the quantification of nanodomains.
f. Finally overlay the STED image. One can now see the correlation between PALM and STED images before and after transformation (Figure 6D).

Note: As a positive control, we electroporated mEos3.2-actin in place of Xph20-mEos3.2, expecting a good match with the corresponding GFP-actin signal. When the correlative PALM-STED protocol is done on neurons co-expressing mEos3.2-actin and GFP-actin, an excellent super-imposition between the PALM and STED signals after image correlation is observed (Figures 6E and 6F). Because actin filaments form a branched network that fill the whole dendritic spine structure,[19–21] no particular organization in nanodomains is expected there.

EXPECTED OUTCOMES

The raw outputs of the protocol are: i) the SMLM localization files of specific proteins within sub-cellular compartments of the cells under study (here dendritic spines in neurons), and ii) the reconstructed super-resolved images of protein distribution correlated with the images obtained in STED. These files can further be used to generate quantitative data, e.g., correlations between the number and size of specific protein nanodomains versus the size of the sub-cellular structures, as detailed below. Specifically, we found that individual dendritic spines identified in STED contained from 0 to 4 discrete PSD-95 nanodomains detected in PALM (Figures 6G and 6H). Those nanodomains had a relatively constant surface area, independently of their actual number in the

spine, but the number of nanodomains was positively correlated with the projected area of the dendritic spines (Figure 6I), as previously reported.[1,22–24] This specific architecture of synapses in punctate nano-domains or -modules seems to be crucial in their response to plasticity mechanisms.[22,25]

This protocol can easily be applied to study other synaptic targets including adhesion or cytoskeletal proteins, for example N-cadherin and the WAVE complex, that have been successfully tagged with mEos3.2 for PALM.[6,19,] These data might be used in the future to establish an overall atlas of protein nanoscale organization in reference to dendritic spine morphology.

In cases where mEos3.2 fusion proteins are not available or functional, the PALM procedure described here can readily be replaced by dSTORM performed on neurons stained with appropriate primary and dye-conjugated antibodies.[26–28] Moreover, the analysis of dSTORM data using PALMTracer or ThunderSTORM is very similar to that used for PALM. dSTORM can be implemented on the same type of microscope used for PALM provided it is equipped with powerful lasers (> 500 mW) to bring fluorophores such as Alexa Fluor 532 or 647 into the stochastic emission mode. One would then have to adjust the combination of stainings and fluorophores between the two microscopy modes (e.g., Alexa532 in dSTORM and Atto-647N in STED, or Alexa647 in dSTORM and Alexa532 in STED). Our preliminary experiments indicate that it is indeed possible to perform such correlative dSTORM-STED imaging using the same overall protocol.

QUANTIFICATION AND STATISTICAL ANALYSIS

Our quantification consists in: i) identifying spine heads on STED images and measuring their surface area; ii) determining the number and area of PSD-95 nanodomains from PALM images in these spines; and iii) correlating both types of information. The projected surface area of spine heads was measured on STED images using Fiji (Figures 4C–4E). Thanks to actin accumulation in spine heads, a simple intensity threshold was used to determine spine head surface area, and to record the regions around these spines. On PALM images, the transformed localization file corresponding to single Xph20-mEos3.2 fusion proteins was uploaded in SR-Tesseler software[10,29] to perform segmentation and quantification of the PSD-95 nanodomains (Figure 4F). After construction of the Voronoï diagram, a local density factor of 4 was applied to segment PSD-95 nano-domains. Finally, spine regions identified on STED images were also imported in SR-Tesseler to extract for each individual spine the number of PSD-95 nano-domains. 105 dendritic spines from 7 independent neurons were analyzed and histograms were plotted (Figure 4G). No quantification was made on the localizations of mEos3.2-actin given its fairly uniform distribution in the spine head.

LIMITATIONS

When compared to the original PALM-STED correlation protocol published previously,[1] this protocol using two different microscopes cannot accommodate live samples. The first reason is that one has to move the sample between the two microscopes. The second reason is that amplification of the GFP-actin signal for STED requires cell fixation followed by immunocytochemistry. Moreover, because the number of wavelengths we can use throughout the procedure is limited to 4, and that PALM already uses two channels (405 nm for photoconversion of mEos3.2 and 561 nm to excite the red-shifted form of mEos3.2), we can image only one mEos3.2 tagged protein at a time. So the PALM procedure has to be repeated for each protein (here Xph20-mEos3.2 and mEos3.2-actin), in reference to the GFP-actin signal which is later imaged in STED after amplification. In addition, some synaptic proteins might be more difficult to fuse to large tags such as mEos3.2 that can affect their folding or localization. In that case, one might prefer to perform dSTORM with antibodies to native proteins or to recombinant proteins bearing smaller tags,[26–28] as mentioned above. Finally, regarding synapse morphology imaged in STED, although we chose to express GFP-actin in neurons as a robust marker of dendritic spines, and we previously checked

that GFP-actin is expressed only 10% in excess of endogenous actin stained with antibodies,[30] there is always a risk that GFP-actin over-expression affects spine morphology. In that case, one might prefer to express a neutral volume marker such as GFP, although it is not specifically enriched in spines.

TROUBLESHOOTING

Problem 1

Related to Section "dissection, electroporation and culture of primary neurons" (before you begin, Steps 7–11). The primary neurons appear scarce, unhealthy, or underdeveloped, and/or other non-neuronal cell types are present on the coverslips.

Potential solutions

- If neurons seem not to be numerous enough, it may be that cell counting after the dissection was not accurate, or that electroporation was harmful. Adjust the settings on the electroporation machine by selecting the "high viability" criterion. One might also consider adding more non-electroporated neurons to the culture to favor development.
- The presence of cell types other than neurons may be due to incomplete removal of the meninges (before you begin, Step 8b), that has allowed microglial cells to proliferate on the coverslips, thereby altering neuronal development. Repeat the dissection by taking this important aspect into consideration.
- Another possibility is that glial cells have not proliferated enough on the underlying plastic dish (before you begin, Step 5), and thereby do not form the 80-90% confluent monolayer that is required to provide neurons with sufficient nutrients and growth factors. Pay attention that glial dishes are well covered by astrocytes before introducing the coverslips containing neurons. Alternatively, thaw a previously frozen vial of glial cells and culture them to 80-90% confluence.

Problem 2

Related to Section "acquisition of PALM data" (Steps 12–13). When observing the electroporated neurons plated on etched coverslips for the first time, the patterns appear upside down.

Potential solution

- This is due to the fact that neurons were seeded on the wrong side of the coverslip. Observe the coverslips carefully with a shelf microscope and place them on the right side in the 60 mm dish before placing the paraffin dots and plating the neurons. (See Before you begin, Step 1.g).

Problem 3

Related to sections "acquisition of PALM data" (Step 15) and "STED acquisition" (Steps 27–28). The fluorescence signal in one or the other microscopy mode is too weak to be exploited.

Potential solution

- A first explanation that applies to both PALM and STED is that there is a poor expression of the proteins of interest after electroporation. Plasmids used for electroporation may degrade over time, and it might be useful to make fresh preparations once in a while. Alternatively, one might want to use different methods for plasmid delivery into neurons, such as transfection with cationic liposomes or calcium phosphate precipitates based on published protocols. These methods traditionally lead to a stronger protein expression in neurons, but can also be more harmful to the cells.
- A second explanation specific to PALM is that there is not a good detection of photo-converted mEos3.2 fusion proteins. Since laser alignment may move over time, check the laser intensity at the objective front lens using a power meter, for both the 405 nm and 561 nm lines. The 405 nm laser power has to be sufficient for proper mEos3.2 photo-conversion, and the 561 nm

laser power has to be high enough to allow for a good detection of the mEos3.2 signal above the background. Also check the various optical components of the microscope (e.g., dirty objective, wrong dichroic mirror and/or emission filter, unwanted presence of neutral density filters in the optical path) that may interfere with excitation or emission light. Finally play on the TIRF angle and focus position to optimize the signal to noise ratio of single molecules. The Tetraspeck beads can serve here as positive controls.

- A third explanation which applies specifically to STED is that there was an issue with the immunocytochemistry procedure, e.g., the antibodies are not concentrated enough or might have degraded over time. We recommend to aliquot the primary and secondary antibodies in small volumes, so as to take a fresh aliquot for every new experiment, and thereby avoid repeated cycles of freezing and thawing. One might also want to optimize the antibody source and dilution to get the strongest and most specific signals as possible from electroporated cells.

Problem 4

Related to the Section "PALM-STED image correlation" (Steps 34–35). The SMLM and STED images appear rotated with respect to each other.

Potential solution

- This is due to the fact that the etched coverslip is slightly moving within the holding chamber. Use a holding chamber that allows a perfect grip of the coverslip to minimize a potential rotation. This is achieved by letting just enough space for the 18 mm square coverslips to fit in the chamber. In practice, given the intrinsic size variability of the coverslips (i.e., from 17.9 to 18.2 mm), the cutout was a square of 18.4 mm.

Problem 5

Related to the Section "PALM-STED image correlation" (Steps 34–35). The quality of the correlation between SMLM and STED signals is not uniform across all regions of the image.

Potential solution

- This is likely due to the fact that the correlation matrix is imperfect, since only a small number of beads are matched to one another in the two microscopy modes. Some beads may be also missed in one or the other mode because of different imaging depths between techniques.
- Increase the number of Tetraspeck beads on each image by adjusting the concentration of beads put on the sample before the SMLM experiment. There should be at least 10 beads per field of view, but having too many beads (> 20) is also not ideal because they might bind to neurons and thereby contaminate the intrinsic signal of mEos3.2 fusion proteins acquired in PALM.
- Acquire a z-stack of beads in the two microscopy modes to make sure that all beads are captured, and make a maximal z-projection.

RESOURCE AVAILABILITY

Lead contact

Further information and requests for resources and reagents should be directed to and will be fulfilled by the lead contact, Olivier Thoumine (Olivier.thoumine@u-bordeaux.fr).

Technical contact

Further information on methodological details should be directed to and will be fulfilled by the technical contact, Tiffany Cloâtre (tiffany.cloatre@u-bordeaux.fr).

Materials availability

This study did not generate new or unique reagents.

Data and code availability

Part of the figures were created with BioRender (biorender.com), using an individual license.

- The protocol includes all experimental datasets generated or analyzed during this study.
- Microscopy data reported in this paper will be shared by the lead contact upon request.
- Any additional information required to reanalyze the data reported in this paper is available from the lead contact upon request.
- All original code for napari-beadreg and PoCA (which includes the SR-Tesseler method) has been deposited at GitHub and Zenodo and is publicly available as of the date of publication. DOIs are listed in the key resources table. More information on the software can directly be asked to the author F.L.
- The computer software used to analyze single molecule localizations (PALMTracer) can be made available upon request to the author J.-B.S.

SUPPLEMENTAL INFORMATION

Supplemental information can be found online at https://doi.org/10.1016/j.xpro.2024.103160.

ACKNOWLEDGMENTS

This research was supported by grants from the French Agence Nationale de la Recherche (ANR-20-CE11-0006-01 "NanoSynAtlas" to F.L. and O.T. and ANR-21-CE11-0019-01 "Synaptoligation" to O.T.). STED microscopy was done at the Bordeaux Imaging Center, part of the France-BioImaging national infrastructure (grant ANR-10-INBS-04-0). The Cell Biology Facility of our institute is partly funded by grants from the University of Bordeaux (GPR BRAIN_2030).

The authors thank the IINS Cell Biology Facility, especially E. Verdier, A. Caralp, N. Retailleau, M. Meras, and D. Bouchet, for primary neuron cultures; R. Sterling, A. Castets, and Z. Andrieux for logistics; A. Kechkar and C. Butler (IINS) for the PALMTracer single-molecule detection program; M. Sainlos and D. Choquet (IINS) for the gifts of mEos3.2-actin and Xph20-mEos3.2; A. Matus (FMI, University of Basel) for the gift of GFP-actin; C. Desquines and B. Tessier (IINS) for molecular biology; and members of the Thoumine team for scientific insight.

AUTHOR CONTRIBUTIONS

T.C. performed experiments, analyzed the data, and made the figures; M.M. and O.T. supervised the technical workflow; O.T. and F.L. conceptualized the project and provided funding. F.L. and J.-B.S. provided dedicated software. All authors participated in the writing and editing of the manuscript.

DECLARATION OF INTERESTS

The authors declare no competing interests.

REFERENCES

1. Inavalli, V.V.G.K., Lenz, M.O., Butler, C., Angibaud, J., Compans, B., Levet, F., Tønnesen, J., Rossier, O., Giannone, G., Thoumine, O., et al. (2019). A super-resolution platform for correlative live single-molecule imaging and STED microscopy. Nat. Methods *16*, 1263–1268. https://doi.org/10.1038/s41592-019-0611-8.

2. Kaech, S., and Banker, G. (2006). Culturing hippocampal neurons. Nat. Protoc. *1*, 2406–2415. https://doi.org/10.1038/nprot.2006.356.

3. Fischer, M., Kaech, S., Wagner, U., Brinkhaus, H., and Matus, A. (2000). Glutamate receptors regulate actin-based plasticity in dendritic spines. Nat. Neurosci. *3*, 887–894. https://doi.org/10.1038/78791.

4. Rimbault, C., Maruthi, K., Breillat, C., Genuer, C., Crespillo, S., Puente-Muñoz, V., Chamma, I., Gauthereau, I., Antoine, S., Thibaut, C., et al. (2019). Engineering selective competitors for the discrimination of highly conserved protein-protein interaction modules. Nat. Commun. *10*, 4521. https://doi.org/10.1038/s41467-019-12528-4.

5. Rimbault, C., Breillat, C., Compans, B., Toulmé, E., Vicente, F.N., Fernandez-Monreal, M., Mascalchi, P., Genuer, C., Puente-Muñoz, V., Gauthereau, I., et al. (2024). Engineering paralog-specific PSD-95 recombinant binders as minimally interfering multimodal probes for advanced imaging techniques. Elife *13*, e69620–e69637. https://elifesciences.org/articles/69620. https://doi.org/10.7554/eLife.69620.

6. Garcia, M., Leduc, C., Lagardère, M., Argento, A., Sibarita, J.-B., and Thoumine, O. (2015). Two-tiered coupling between flowing actin and immobilized N -cadherin/catenin complexes in neuronal growth cones. Proc. Natl. Acad. Sci. USA *112*, 6997–7002. https://doi.org/10.1073/pnas.1423455112.

7. Mondin, M., Tessier, B., and Thoumine, O. (2013). Assembly of Synapses: Biomimetic Assays to Control Neurexin/Neuroligin

Interactions at the Neuronal Surface. Curr. Protoc. Neurosci. *Chapter 2*, Unit.2.19. https://doi.org/10.1002/0471142301.ns0219s64.

8. Schneider, C.A., Rasband, W.S., and Eliceiri, K.W. (2012). NIH Image to ImageJ: 25 years of image analysis. Nat. Methods *9*, 671–675. https://doi.org/10.1038/nmeth.2089.

9. Ovesný, M., Křížek, P., Borkovec, J., Švindrych, Z., and Hagen, G.M. (2014). ThunderSTORM: A comprehensive ImageJ plug-in for PALM and STORM data analysis and super-resolution imaging. Bioinformatics *30*, 2389–2390. https://doi.org/10.1093/bioinformatics/btu202.

10. Levet, F., Hosy, E., Kechkar, A., Butler, C., Beghin, A., Choquet, D., and Sibarita, J.-B. (2015). SR-Tesseler: a method to segment and quantify localization-based super-resolution microscopy data. Nat. Methods *12*, 1065–1071. https://doi.org/10.1038/nmeth.3579.

11. Levet, F., and Sibarita, J.B. (2023). PoCA: a software platform for point cloud data visualization and quantification. Nat. Methods *20*, 629–630. https://doi.org/10.1038/s41592-023-01811-4.

12. Izeddin, I., Boulanger, J., Racine, V., Specht, C.G., Kechkar, A., Nair, D., Triller, A., Choquet, D., Dahan, M., and Sibarita, J.B. (2012). Wavelet analysis for single molecule localization microscopy. Opt Express *20*, 2081–2095. https://doi.org/10.1364/OE.20.002081.

13. Kechkar, A., Nair, D., Heilemann, M., Choquet, D., and Sibarita, J.-B. (2013). Real-time analysis and visualization for single-molecule based super-resolution microscopy. PLoS One *8*, e62918. https://doi.org/10.1371/journal.pone.0062918.

14. Nair, D., Hosy, E., Petersen, J.D., Constals, A., Giannone, G., Choquet, D., and Sibarita, J.-B. (2013). Super-Resolution Imaging Reveals That AMPA Receptors Inside Synapses Are Dynamically Organized in Nanodomains Regulated by PSD95. J. Neurosci. *33*, 13204–13224. https://doi.org/10.1523/JNEUROSCI.2381-12.2013.

15. Butler, C., Saraceno, G.E., Kechkar, A., Bénac, N., Studer, V., Dupuis, J.P., Groc, L., Galland, R., and Sibarita, J.-B. (2022). Multi-Dimensional Spectral Single Molecule Localization Microscopy. Front. Bioinform. *2*, 813494–813514. https://doi.org/10.3389/fbinf.2022.813494.

16. Duchon, J. (1977). Splines minimizing rotation-invariant semi-norms in Sobolev spaces. In Constructive Theory of Functions of Several Variables, K.Z. Walter Schempp, ed. (Berlin, Heidelberg: Springer), pp. 85–100. https://doi.org/10.1007/BFb0086566.

17. Manley, S., Gillette, J.M., Patterson, G.H., Shroff, H., Hess, H.F., Betzig, E., and Lippincott-Schwartz, J. (2008). High-density mapping of single-molecule trajectories with photoactivated localization microscopy. Nat. Methods *5*, 155–157. https://doi.org/10.1038/nmeth.1176.

18. Rossier, O., Octeau, V., Sibarita, J.B., Leduc, C., Tessier, B., Nair, D., Gatterdam, V., Destaing, O., Albigès-Rizo, C., Tampé, R., et al. (2012). Integrins β 1 and β 3 exhibit distinct dynamic nanoscale organizations inside focal adhesions. Nat. Cell Biol. *14*, 1057–1067. https://doi.org/10.1038/ncb2588.

19. Chazeau, A., Mehidi, A., Nair, D., Gautier, J.J., Leduc, C., Chamma, I., Kage, F., Kechkar, A., Thoumine, O., Rottner, K., et al. (2014). Nanoscale segregation of actin nucleation and elongation factors determines dendritic spine protrusion. EMBO J. *33*, 2745–2764. https://doi.org/10.15252/embj.201488837.

20. Honkura, N., Matsuzaki, M., Noguchi, J., Ellis-Davies, G.C.R., and Kasai, H. (2008). The subspine organization of actin fibers regulates the structure and plasticity of dendritic spines. Neuron *57*, 719–729. https://doi.org/10.1016/j.neuron.2008.01.013.

21. Frost, N.A., Shroff, H., Kong, H., Betzig, E., and Blanpied, T.A. (2010). Single-molecule discrimination of discrete perisynaptic and distributed sites of actin filament assembly within dendritic spines. Neuron *67*, 86–99. https://doi.org/10.1016/j.neuron.2010.05.026.

22. Hruska, M., Henderson, N., Le Marchand, S.J., Jafri, H., and Dalva, M.B. (2018). Synaptic nanomodules underlie the organization and plasticity of spine synapses. Nat. Neurosci. *21*, 671–682. https://doi.org/10.1038/s41593-018-0138-9.

23. Nozawa, K., Sogabe, T., Hayashi, A., Motohashi, J., Miura, E., Arai, I., and Yuzaki, M. (2022). In vivo nanoscopic landscape of neurexin ligands underlying anterograde synapse specification. Neuron *110*, 3168–3185.e8. https://doi.org/10.1016/j.neuron.2022.07.027.

24. Fukata, Y., Dimitrov, A., Boncompain, G., Vielemeyer, O., Perez, F., and Fukata, M. (2013). Local palmitoylation cycles define activity-regulated postsynaptic subdomains. J. Cell Biol. *202*, 145–161. https://doi.org/10.1083/jcb.201302071.

25. Tang, A.-H., Chen, H., Li, T.P., Metzbower, S.R., MacGillavry, H.D., and Blanpied, T.A. (2016). A trans-synaptic nanocolumn aligns neurotransmitter release to receptors. Nature *536*, 210–214. https://doi.org/10.1038/nature19058.

26. Beghin, A., Kechkar, A., Butler, C., Levet, F., Cabillic, M., Rossier, O., Giannone, G., Galland, R., Choquet, D., and Sibarita, J.B. (2017). Localization-based super-resolution imaging meets high-content screening. Nat. Methods *14*, 1184–1190. https://doi.org/10.1038/nmeth.4486.

27. Lagardère, M., Drouet, A., Sainlos, M., and Thoumine, O. (2022). High-Resolution Fluorescence Imaging Combined With Computer Simulations to Quantitate Surface Dynamics and Nanoscale Organization of Neuroligin-1 at Synapses. Front. Synaptic Neurosci. *14*, 835427. https://doi.org/10.3389/fnsyn.2022.835427.

28. Chamma, I., Levet, F., Sibarita, J.-B., Sainlos, M., and Thoumine, O. (2016). Nanoscale organization of synaptic adhesion proteins revealed by single-molecule localization microscopy. Neurophotonics *3*, 041810. https://doi.org/10.1117/1.NPh.3.4.041810.

29. Levet, F., Julien, G., Galland, R., Butler, C., Beghin, A., Chazeau, A., Hoess, P., Ries, J., Giannone, G., and Sibarita, J.B. (2019). A tessellation-based colocalization analysis approach for single-molecule localization microscopy. Nat. Commun. *10*, 2379–2412. https://doi.org/10.1038/s41467-019-10007-4.

30. Chazeau, A., Garcia, M., Czöndör, K., Perrais, D., Tessier, B., Giannone, G., and Thoumine, O. (2015). Mechanical coupling between transsynaptic N-cadherin adhesions and actin flow stabilizes dendritic spines. Mol. Biol. Cell *26*, 859–873. https://doi.org/10.1091/mbc.e14-06-1086.